Numerical analysis of long-range spatial correlations in surface growth

Hui Xia[*] and Gang Tang[†]

Department of Physics, China University of Mining and Technology, Xuzhou 221116, China

Yueheng Lan[‡]

Department of Physics, Beijing University of Posts and Telecommunications, Beijing 100876, China

To analyze long-range spatial correlations in surface growth, we study numerically a class of generalized Kardar-Parisi-Zhang equation with a fractional Laplacian and driven by long-range spatially correlated noise, and investigate interplay of the fractional Laplacian and correlated noise. We find that the growth system with long-range correlation exhibits nontrivial scaling properties, such as strong dependence on the noise correlation and weak dependence on the fractional order. The growth instability is also discussed in various parameter regimes.

I. INTRODUCTION

Disordered surface growth in nonequilibrium conditions has received much attention in the last several decades because it is related to various physical phenomena such as crystal growth, bacterial growth, molecular beam epitaxy (MBE), fluid flows in porous media, and fracture cracks, among others [1–4]. In this field, special efforts focus on relating discrete microscopic growth models to their corresponding continuum field theories. The first nonlinear continuum equation used to study the growth of an interface is the well-known Kardar-Parisi-Zhang (KPZ) equation [5], which describes the dynamics of an interface with environmental noise. The KPZ model has become a paradigm for the study of kinetic roughening and makes up a distinct universality class in dynamic phase transition. In the (1+1) dimension, the KPZ equation reads

$$\frac{\partial h}{\partial t} = \nu \nabla^2 h + \frac{\lambda}{2}(\nabla h)^2 + \eta(\mathbf{x},t), \tag{1}$$

where the first term on the right-hand side is the diffusion term, the second one is the nonlinear term describing the lateral growth, and $\eta(\mathbf{x},t)$ is a noise term which represents a stochastic process.

The study of growing surfaces is often characterized by fluctuations of the growth height around its mean value. One of the most important physical quantities describing surface roughening is the global interfacial width $W(L,t)$, which is defined as

$$W(L,t) \equiv \frac{1}{\sqrt{L}} \langle \overline{[h(\mathbf{x},t) - \overline{h}(t)]^2} \rangle^{1/2}, \tag{2}$$

where $\bar{h}_L$ denotes the spatial average in a system with size L, and $\langle \cdots \rangle$ stands for the average over noise realizations. In many cases, starting from a flat surface, the global width has a dynamic scaling form of Family-Vicsek type [6],

$$W(L,t) = t^\beta f(L/t^{1/z}), \tag{3}$$

where the scaling function $f(x) \sim x^\alpha$ for $x \ll 1$ and $f(x) \to$ const for $x \gg 1$. The roughness exponent α is a critical exponent that characterizes the roughness of the saturated interface, and the dynamic exponent z describes the dependence of the crossover time on the system size through the relation $t_x \sim L^z$. The ratio $\beta = \alpha/z$ is called the growth exponent and describes the short time behavior of the surface.

Nevertheless, the local growth assumption is not always justified physically. Few experiments were able to give the KPZ exponents directly, but an overwhelming majority of experimental investigations have reported values of scaling exponents inconsistent with the local KPZ class [1–3]. The discrepancy has spurred considerable theoretical activities involving modifications of the KPZ model [7]. Meanwhile, in most experimentally studied growth systems, it is believed that long-range correlations or nonlocal effects are present in reality, although they can be very weak under certain circumstances. It is, therefore, important to understand how the behavior of surface growth would be modified when the long-range correlations are taken into account. To our knowledge, there are three kinds of modified KPZ models that account for long-range spatial correlations, namely, the KPZ equation in the presence of spatially correlated noise [8–11], the nonlocal KPZ equation [12–14], and the KPZ equation with a fractional Laplacian for describing anomalous diffusion [15,16]. Since both a space-fractional Laplacian and spatially correlated noise can describe nonlocal effects, it is natural to consider how interplay between them affects the scaling properties in surface roughening. In this work, to investigate the dynamic scaling of surface growth with long-range interactions, we study numerically the time evolution of the generalized KPZ equation with a fractional Laplacian and long-range spatially correlated noise. The scaling exponents obtained from numerical computation are consistent with the results based on analytical approaches. This work shows that long-range spatial correlations affect scaling behavior of the surface growth.

The rest of this paper is organized as follows. First, we describe the fractional KPZ (FKPZ) equation, and its linearization, the fractional Edwards-Wilkinson (FEW) equation. Next we present numerical methods and simulation results in the (1+1) dimension. Finally we discuss the obtained results and conclude.

―――――――

[*]hxia@cumt.edu.cn

[†]gangtang@cumt.edu.cn

[‡]lanyh@bupt.edu.cn

II. THE FRACTIONAL GROWTH EQUATIONS

The modified KPZ equation is obtained from the local KPZ equation by replacing the standard second-order spacial derivative with a fractional Laplacian operator [15,16], which can be posed as

$$\frac{\partial h}{\partial t} = \nu \Delta_\gamma h(x,t) + \frac{\lambda}{2}(\nabla h)^2 + \eta(\mathbf{x},t). \quad (4)$$

Here, $\Delta_\gamma h \equiv -(-\Delta)^{\gamma/2}(1 < \gamma \leqslant 2)$ is the fractional Laplacian. It can be defined as the Riesz-type fractional derivative [17],

$$
\begin{aligned}
\Delta_\gamma h(x,t) &= -(-\Delta)^{\gamma/2} h(x,t) \\
&= -[C_+(\gamma)_x D_+^\gamma h(x,t) + C_-(\gamma)_x D_-^\gamma h(x,t)], \quad (5)
\end{aligned}
$$

where $C_+ = C_- = 1/[2\cos(\pi\gamma)]$, and $_x D_+^\gamma h(x,t)$ and $_x D_-^\gamma h(x,t)$ denote the left and right Grunwald-Letnikov fractional derivatives, respectively:

$$_x D_+^\gamma h(x,t) = \lim_{\Delta x \to 0}(\Delta x)^{-\gamma} \sum_{k=0}^{(x-a)/\Delta x} g_k h(x - k\Delta x, t),$$

$$_x D_-^\gamma h(x,t) = \lim_{\Delta x \to 0}(\Delta x)^{-\gamma} \sum_{k=0}^{(L-x)/\Delta x} g_k h(x - k\Delta x, t), \quad (6)$$

where $g_0 = 1$, $g_k = (-1)^k \frac{\gamma(\gamma-1)\cdots(\gamma-k+1)}{k!}$ $(k = 1,2,3,\ldots)$, a is the lattice spacing, and L is the system size in our context. $\eta(x,t)$ is a spatially correlated noise described by $\langle\eta(x,t)\rangle = 0$ and $\langle\eta(\mathbf{x},t)\eta(\mathbf{x}',t')\rangle = 2D|\mathbf{x} - \mathbf{x}'|^{2\sigma-d}\delta(t - t')$, where the coefficient D is the strength of noise, d is the dimension of the growth substrate, and σ is the spatial correlation index. As a special case in which $\gamma = 2$ and $\sigma = 0$, Eq. (4) corresponds to the local KPZ equation driven by Gaussian white noise.

The FKPZ equation was proposed first by Mann and Woyczynski [15], who suggested a fractal Langevin-type equation for growing fractal interfaces in the presence of self-similar hopping surface diffusion in order to explain the related experiments [18], where impurities exist on the growing surface, and the standard KPZ equation loses its validity, and then a fractional Laplacian was introduced into the continuum equation (1) describing another relaxation mechanism. Katzav [16] generalized the FKPZ equation by introducing spatially correlated noise and investigated the scaling behavior of the FKPZ equation based on a self-consistent expansion (SCE) approach [19].

For $\lambda = 0$, Eq. (4) reduces to the FEW equation and therefore can be solved exactly [4,15]. The scaling exponents in this case can also be obtained easily through a power-counting analysis [1]: The scale transformation $x \to bx$, together with the corresponding rescaling in the height $h \to b^\alpha h$, the time $t \to b^z t$, and the noise $\eta(x,t) \to b^{-(d+z-2\sigma)/2}\eta(x,t)$, transforms Eq. (4) to

$$b^{\alpha-z}\frac{\partial h}{\partial t} = \nu b^{\alpha-\gamma}\Delta_\gamma h(x,t) + b^{-(d+z-2\sigma)/2}\eta(\mathbf{x},t). \quad (7)$$

Multiplying both sides of Eq. (7) with $b^{z-\alpha}$, we obtain

$$\frac{\partial h}{\partial t} = \nu b^{z-\gamma}\Delta_\gamma h(x,t) + b^{\sigma-\alpha-(d-z)/2}\eta(\mathbf{x},t). \quad (8)$$

In order to have scale invariance we must set the exponent of b equal to zero, which results in $\alpha = (\gamma + 2\sigma - d)/2$, $\beta = (\gamma + 2\sigma - d)/2\gamma$, and $z = \gamma$. For $\gamma = 2$ and $\sigma = 0$, $\alpha = (2 - d)/2$, $\beta = (2 - d)/4$, and $z = 2$, which are the exact values of the local Edwards-Wilkinson (EW) equation with Gaussian white noise [20]. In the case of the (1+1)-dimensional FEW equation, $\alpha = (\gamma - 1)/2$, $\beta = (\gamma - 1)/2\gamma$, and $z = \gamma$.

For $\lambda \neq 0$, the nonlinear term in Eq. (4) is in fact relevant and, therefore, affects the scaling exponents [15,16]. Similar to the scale transformation in the linear case, we could transform Eq. (4) to

$$
\begin{aligned}
b^{\alpha-z}\frac{\partial h}{\partial t} &= \nu b^{\alpha-\gamma}\Delta_\gamma h(x,t) + \frac{\lambda}{2}b^{2\alpha-2}(\nabla h)^2 \\
&\quad + b^{-(d+z-2\sigma)/2}\eta(\mathbf{x},t). \quad (9)
\end{aligned}
$$

Multiplying both sides of Eq. (9) with $b^{z-\alpha}$, we obtain

$$
\begin{aligned}
\frac{\partial h}{\partial t} &= \nu b^{z-\gamma}\Delta_\gamma h(x,t) + \frac{\lambda}{2}b^{\alpha+z-2}(\nabla h)^2 \\
&\quad + b^{\sigma-\alpha-(d-z)/2}\eta(\mathbf{x},t). \quad (10)
\end{aligned}
$$

To ensure scaling invariance, one would expect naively that the right-hand side of Eq. (10) must be independent of b. However, this procedure provides three scaling relations for two exponents, thereby overdetermining them. The assumption that the coefficient of the nonlinear term of Eq. (10) should be independent of scaling leads to the scaling relation $\alpha + z = 2$, which implies that the FKPZ equation has the same superscaling relation as the standard KPZ equation [1].

In order to investigate analytically the scaling properties of the FKPZ equation driven by spatially correlated noise, Katzav [16] developed the SCE approach, which yields rich phases of the FKPZ system. When the spatial correlation parameter $\sigma \neq 0$, there is a weak-coupling solution with critical exponents $\alpha = (\gamma + 2\sigma - d)/2$, $\beta = (\gamma + 2\sigma - d)/2\gamma$, and $z = \gamma$. When $\sigma = 0$, the scaling exponents naturally restore the values of the FEW with Gaussian white noise (they are called weak coupling because they are exactly the solutions obtained in the case of the FEW equation discussed above). The second type of solution is the strong-coupling solution that obeys the well-known scaling relation $\alpha + z = 2$, including three special cases: (i) independent of the noise correlation parameter and the fractional order, $\alpha = (\Gamma_0(d) - d)/2$, $\beta = (\Gamma_0(d) - d)/(d - \Gamma_0(d) + 4)$, and $z = (d - \Gamma_0(d) + 4)/2$, where $\Gamma_0(d)$ is the steady state value and only depends on the substrate dimension d, more specifically, $\Gamma_0(1) = 2$, and $\Gamma_0(2) = 2.59$; (ii) independent of the fractional order but dependent on the noise correlation parameter, $\alpha = (2\gamma + 2 - d)/3$, $\beta = (2\gamma + 2 - d)/(d + 4 - 2\sigma)$, and $z = (d + 4 - 2\sigma)/3$; and (iii) dependent on the fractional order but independent of the correlation parameter $\alpha = 2 - \gamma$, $\beta = (2 - \gamma)/\gamma$, and $z = \gamma$.

The above-mentioned analytical solutions of the FKPZ system are different evidently in the weak-coupling and the strong-coupling regimes. In the weak-coupling regime, the critical exponents depend on the correlation parameter and the fractional order. However, in the strong-coupling regime the correlation parameter and the fractional order

separately affect the scaling exponents; that is, interplay between the fractional Laplacian and correlated noise is lost. This discrepancy motivated us to check the above results directly in numerical simulations. In the following sections, we give numerical evidences for long-range spatial correlations in these fractional growth systems.

$$\Delta_\gamma h(x,t) = -(-\Delta)^{\gamma/2}h(x,t)$$
$$= -[C_+(\gamma)_x D_+^\gamma h(x,t) + C_-(\gamma)_x D_-^\gamma h(x,t)]$$
$$= -\left[C_+(\gamma)\lim_{\Delta x\to 0}(\Delta x)^{-\gamma}\sum_{k=0}^{(x-a)/\Delta x} g_k h(x-k\Delta x) + C_-(\gamma)\lim_{\Delta x\to 0}(\Delta x)^{-\gamma}\sum_{k=0}^{(L-x)/\Delta x} g_k h(x-k\Delta x) \right]$$
$$= -\frac{1}{2\cos(\pi\gamma/2)(\Delta x)^\gamma}\left[\sum_{k=0}^{(x/\Delta x+1)/\Delta x} g_k h(x-(k-1)\Delta x,t) + \sum_{k=0}^{(x/\Delta x+1)/\Delta x} g_k h(x+(k-1)\Delta x,t) + O(\Delta x) \right]$$
$$\approx -\frac{1}{2\cos(\pi\gamma/2)(\Delta x)^\gamma}\left[\sum_{k=0}^{(x/\Delta x+1)/\Delta x} g_k h(x-(k-1)\Delta x,t) + \sum_{k=0}^{(x/\Delta x+1)/\Delta x} g_k h(x+(k-1)\Delta x,t) \right], \tag{11}$$

which enables rewriting the FKPZ equation with an explicit finite-difference scheme in the following form:

$$\frac{h(x,t+\Delta t)-h(x,t)}{\Delta t} \approx -\frac{1}{2\cos(\pi\gamma/2)(\Delta x)^\gamma}\left[\sum_{k=0}^{(x/\Delta x+1)/\Delta x} g_k h(x-(k-1)\Delta x,t) + \sum_{k=0}^{(x/\Delta x+1)/\Delta x} g_k h(x+(k-1)\Delta x,t) \right]$$
$$+ \frac{\lambda}{(\Delta x)^2}[h(x,t+\Delta t)-h(x,t)]^2/8 + \sigma\left(\frac{12}{\Delta t}\right)^{1/2}\eta(x,t), \tag{12}$$

where $\sigma = (2D/\Delta x)^{1/2}$, and $\eta(i,t)$ is a spatial noise realization at time t with long-range power-law correlation. In order to generate this spatially correlated sequence, we adopt the method by Peng *et al.* [10]. The actual numerical algorithm consists of the following steps: (i) generate a one-dimensional sequence $\eta_0(i,t)$ of uncorrelated random numbers with a Gaussian distribution, (ii) calculate the Fourier coefficients $\eta_0(q,t)$ of the sequence, and obtain $\eta(q,t)$ using $\eta(q,t) = |q|^{-\sigma}\eta_0(q,t)$, and then (iii) implement the inverse Fourier transform back to $\eta(i,t)$, which is the sequence in real space with the desired power-law correlation. In this process, fast Fourier transform is invoked.

In the following simulations, we set the parameters as $\Delta t = 0.05$, $\Delta x = 1$, $\nu = 1$, $\lambda = 4$, $D = 1$, and starting from a flat interface at $t = 0$ with periodic boundary condition. To investigate the scaling behavior of the fractional growth process, we check the time evolution of the interface width $W(L,t)$ in the FKPZ equation at an early time. In Fig. 1, we show double logarithmic plots $W(L,t)$ versus t in a one-dimensional substrate of length $L = 2^n$, with $4 \leqslant n \leqslant 15$ ($16 \leqslant L \leqslant 32768$). We observe clearly the finite-size effect. Here, parameter values $\gamma = 1.75$ and $\sigma = 0.25$ are used.

Figure 1 shows that, for very short times (typically $\log_2 t < 0$), there is a transient region where the initial deposit comes into being. In this region, $W(L,t)$ rapidly increases with t. After this transient, the steady growth begins, and the growth interface is fully driven by the interplay between the fractional Laplacian, the nonlinear lateral correlation, and the correlated noise. Therefore, in a sense, this is where the early growth really starts, and in this regime one is able to

III. NUMERICAL METHODS AND RESULTS

We define $t = i\Delta t$, $i = 1,2,\ldots,m$, $x = k\Delta x$, $k = 1,2,\ldots,n$, where $\Delta t = T/m$ is the step size in time, and $\Delta x = L/n$ is the step size in space. The space-fractional derivative terms in Eq. (5) can be approximated by the scheme [21]

obtain the growth exponent effectively. Then, with increasing growth time, a crossover region is observed, and finally the interface width saturates at the steady-state saturation region. In the steady growth region, we find that, when $L < 512$, the
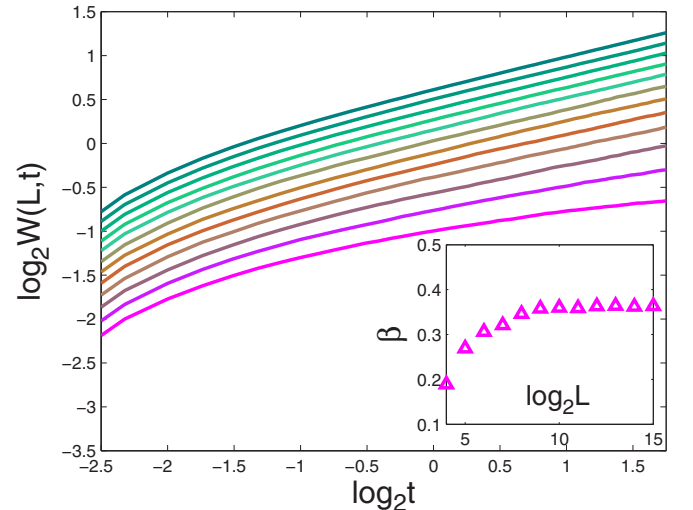

FIG. 1. Log-log plot of the global interfacial width $W(L,t)$ versus time t for the FKPZ equation ($\gamma = 1.75$ and $\sigma = 0.25$) with different system sizes $2^4,\ldots,2^{15}$ (from bottom to top). Results have been averaged over a number of different noise realizations: 5000 for $L = 2^4$, 2500 for $L = 2^5$, 1000 for $L = 2^6$, 750 for $L = 2^7$, 500 for $L = 2^8$, 250 for $L = 2^9$, and 100 for the remaining values of system sizes. The inset shows β as a function of L.
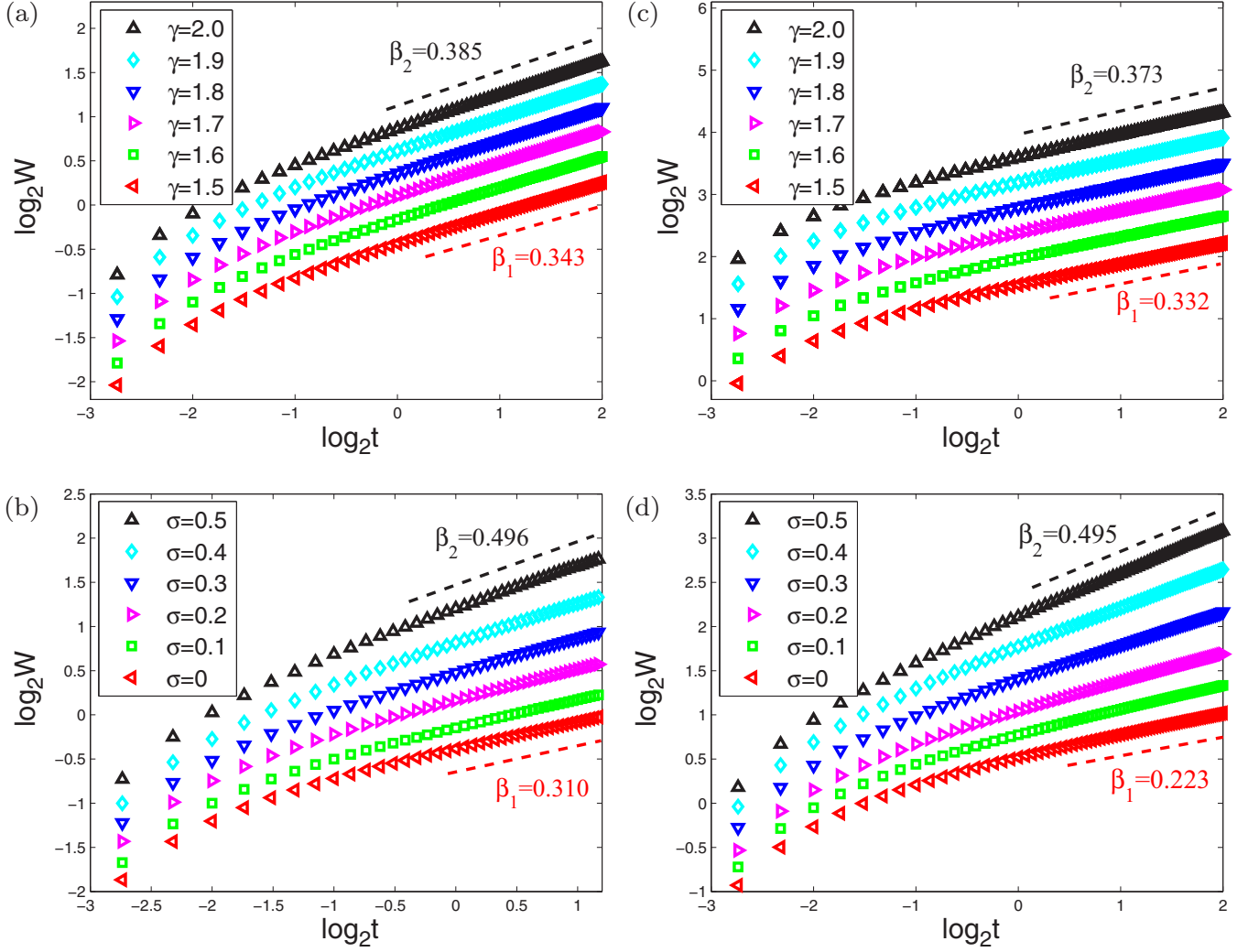
FIG. 2. The log-log plot of the width $W(L,t)$ versus time t for the FKPZ and FEW equations in the short time regime (a) with different γ for the FKPZ equation ($\sigma = 0.25$), (b) with different σ for the FKPZ equation ($\gamma = 1.75$), (c) with different γ for the FEW equation ($\sigma = 0.25$), and (d) with different σ for the FEW equation ($\gamma = 1.75$). In each of these simulations, an average over 100 runs is taken. For the sake of clear comparison, each curve is shifted successively along the vertical coordinate.

slopes (the effective growth exponent) of different systems are different. More precisely, the value of β increases with L monotonously. This suggests a significant finite-size effect of scaling exponents in this discretized fractional growth system. The dependence on system size in the FKPZ equation is similar to that of the local KPZ equation, in which the effective roughness exponent is expected to converge to the asymptotic value as the system size gets large enough. Our simulations show that, in the discretized FKPZ equation, when $L \geqslant 512$, the effective growth exponents for systems with different sizes can be considered approximately equal. In other words, the finite-size effect of scaling exponents could be regarded as trivial beyond this size. The inset of Fig. 1 shows the growth exponent as a function of the system size L ($\gamma = 1.75$ and $\sigma = 0.25$). It indicates that $\beta \simeq 0.364$ for $L \geqslant 512$. Without loss of generality, in the following simulations, we use $L = 8196$ for most of our studies. Very similar results can be obtained with larger values of L.

To describe quantitatively the scaling properties of the FKPZ system, we made the double logarithmic plot of $W(L,t)$ versus t with various fractional orders and spatial correlation parameters. In Fig. 2(a), the fractional order γ is chosen as 1.5–2.0, and the spatial correlation parameter $\sigma = 0.25$. The growth exponents are calculated for different γ using the power-law relation $W \sim t^{\beta}$, and the obtained value is $\beta = 0.343 \sim 0.385$, which weakly depends on γ. Figure 2(b) exhibits a similar power-law relation with $\gamma = 1.75$ and $\sigma(0-0.5)$. In this condition, the growth exponent obviously depends on the spatial correlation coefficient, $\beta = 0.310 \sim 0.496$ when $\sigma = 0-0.5$. Therefore, these results imply that the scaling exponents have weak dependence on the fractional operator and strong dependence on the spatial correlation parameter. In the linear case $\lambda = 0$, the growth exponent changes evidently as γ or σ varies. The numerical results are in agreement with the corresponding analytical values [4,16] [see Figs. 2(c) and 2(d)]. For example, when $\sigma = 0.25$ and $\gamma = 1.5-2.0$, the obtained growth exponent is $\beta = 0.332 \sim 0.373$,
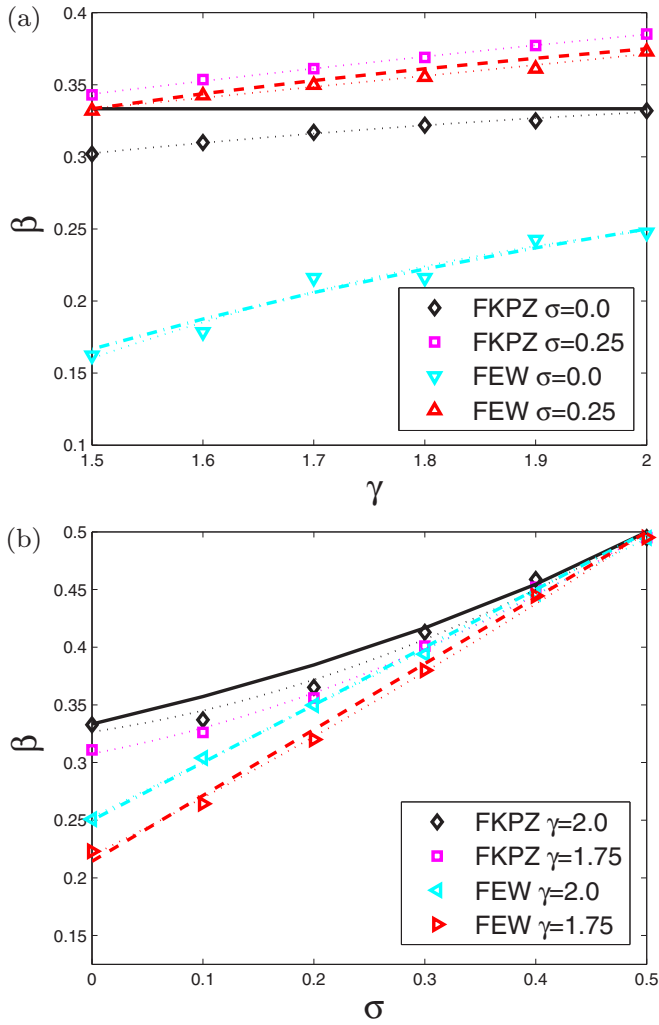
FIG. 3. The growth exponent for the FKPZ and FEW equations in various parameter regimes: (a) β versus γ and (b) β versus σ. The solid, dot-dashed, and dashed lines in (a) indicate the theoretical predictions for the FKPZ ($\gamma = 1.5 - 2.0, \sigma = 0$) [16], FEW ($\gamma = 1.5 - 2.0, \sigma = 0$), and FEW ($\gamma = 1.5 - 2.0, \sigma = 0.25$) equations, respectively; in (b) the corresponding predictions for the FKPZ ($\gamma = 2.0, \sigma = 0 - 0.5$) [9], FEW ($\gamma = 2.0, \sigma = 0 - 0.5$), and FEW ($\gamma = 1.75, \sigma = 0 - 0.5$) equations are solid, dot-dashed, and dashed lines, respectively.

and for $\gamma = 1.75$ and $\sigma = 0$–0.5, $\beta = 0.223 \sim 0.495$. For the special case, $\gamma = 2.0$ and $\sigma = 0$, $\beta \approx 0.25$, which indicates that the linear fractional equation returns to the local EW case [20].

In order to gain more insight into this growth system, it might be interesting to focus on two extreme cases: $\gamma \leqslant 2.0$, $\sigma = 0$ and $\gamma = 2.0$, $\sigma \neq 0$. The first case (namely, $\gamma \leqslant 2.0$ and $\sigma = 0$) corresponds to the FKPZ with Gaussian white noise which is the original equation suggested by Mann and Woyczynski [15]. In this condition, our simulations show that $\beta = 0.302 \sim 0.332$ when $\gamma = 1.5$–2.0 [see Fig. 3(a)]. We find that the dependence on the fractional parameter becomes weaker compared with the case of $\sigma \neq 0$. It implies that the scaling exponents change distinctly by introducing the noise correlation parameter into the fractional KPZ equation; in

other words, the parameters γ and σ affect jointly the scaling behavior of the generalized growth system. These results are well in line with one of the strong-coupling solutions based on the SCE approach [16], and the previous numerical simulations [22] based on the Caputo-type fractional derivative. In this case, the validity condition reads $\Gamma_0(d) > \max\{(d + 4\sigma + 4)/3, (d + 3)/3, d - 2\gamma + 4\}$. The scaling exponents are $z = (d - \Gamma_0(d) + 4)/2$ and $\alpha = (\Gamma_0(d) - d)/2$. More specifically, in the (1+1) dimension, $z = 3/2$ and $\alpha = 1/2$ can be obtained exactly, where the validity condition reads $3/2 \leqslant \gamma \leqslant 2$ [16]. Therefore, the critical exponent is γ independent in the fractional KPZ system with Gaussian white noise.

Interestingly, an inequality on scaling exponents for general dynamical systems has been derived by Katzav and Schwartz [23]. This inequality has been used to successfully estimate the effectiveness and limitation of analytical or numerical approximation in various dynamical growth models. It is not difficult to prove that many analytical methods produce results that violate the dynamical inequality in dealing with nonlocal growth systems. We use the inequality here to check the validity of the numerical results for the FKPZ system and find that the scaling exponents satisfy the exponent inequality when the values of γ range from 1.5 to 2.0.

The second special case (namely, $\gamma = 2.0$ and $\sigma \neq 0$) corresponds to the local KPZ model with spatially correlated noise. This problem has been studied in the past using various analytical approximations, for example, the dynamic renormalization group (DRG) method [8], the scaling approach [9], and SCE [11]. Surprisingly, these analytical tools agree on the basic picture that for a large enough noise parameter one obtains a power-counting strong-coupling solution, given by $\beta = (2\sigma + 1)/(5 - 2\sigma)$. The controversy between different methods lies in the scaling exponents for smaller values of σ, and on the critical value $\sigma_0(= 1/4)$ that separates the two phases. In Fig. 3(b), we provide detailed comparisons of β versus σ for the FKPZ ($\gamma = 2.0$) with the theoretical results. These results show that the scaling exponents we obtained are consistent with the theoretical predictions based on the Flory-type scaling approach [9] and also agree with the previous numerical results from a direct simulation of the KPZ equation driven by spatially correlated noise and the related problem of directed-polymer growth [10].

For the linear FEW equation, the two extreme cases ($\gamma = 2.0$, $\sigma \neq 0$ and $\gamma \neq 2.0$, $\sigma = 0$) correspond to the local EW with spatially correlated noise and the fractional EW equation with Gaussian white noise, respectively. The scaling exponents obtained numerically here are consistent with the corresponding results based on power counting [see Figs. 2(c) and 2(d)]. The results indicate that long-range spatial correlations affect dramatically the scaling behavior of the linear fractional system, and the growth exponent increases monotonously with the correlation parameter γ or σ, which implies that these scaling properties of the linear FEW system differ from those of the nonlinear FKPZ system [16]. Interestingly, we also find that, different from the strong dependence on γ when $\sigma = 0$, the growth exponents in the FEW system driven by the correlated noise ($\sigma \neq 0$) relies only weakly on γ. Therefore, we conclude that, whether in the FKPZ or in the FEW system, the correlated noise and the fractional order combine together to affect the growth
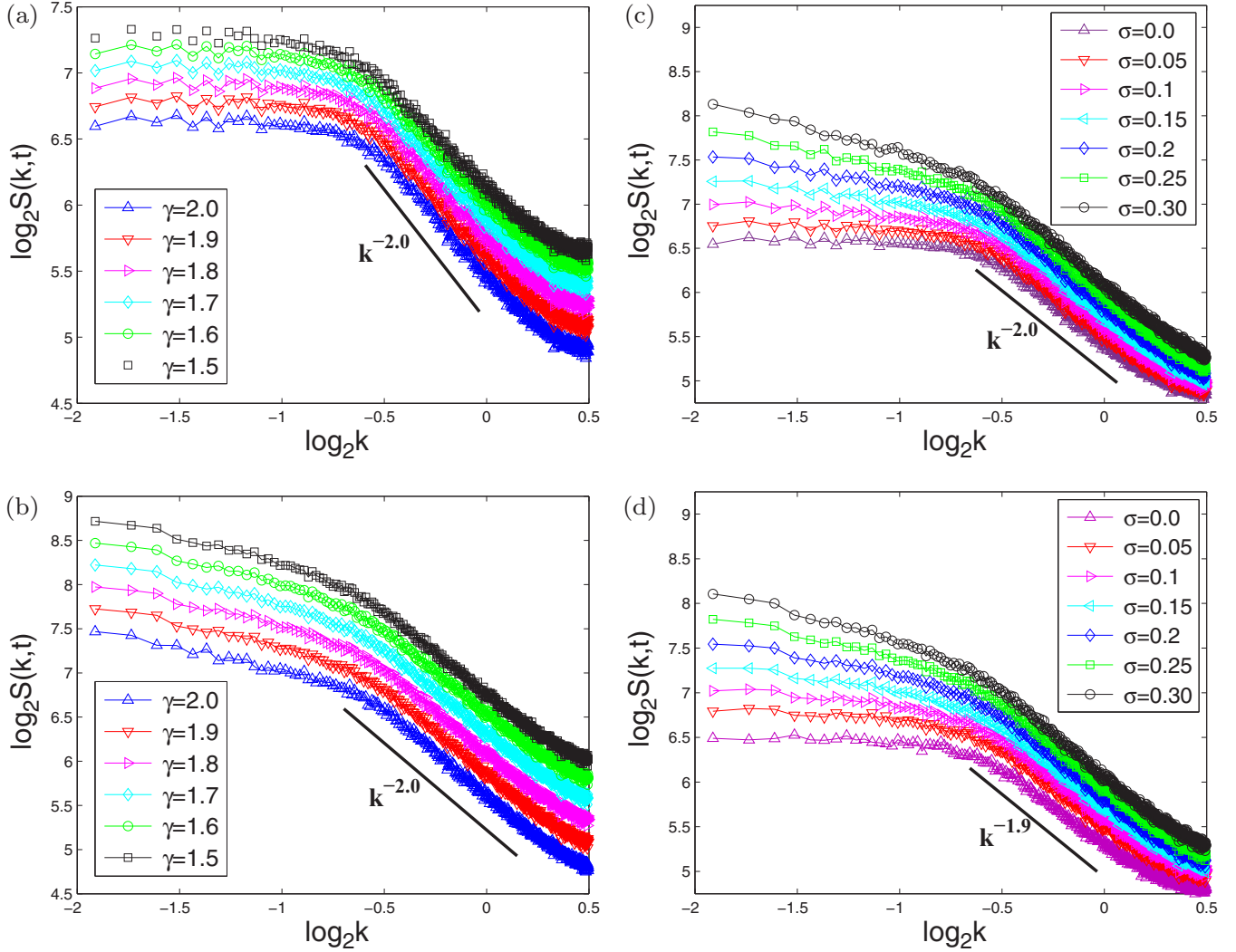
FIG. 4. The log-log plot of the structure factor $S(k,t)$ versus wave number k for the FKPZ equation (a) with different γ and $\sigma = 0$, (b) with different γ and $\sigma = 0.25$, (c) with different σ and $\gamma = 2.0$, and (d) with different σ and $\gamma = 1.75$. In each of these simulations, an average over 250 runs is taken. Every straight line is plotted to guide the eyes. For the sake of clear comparison, each curve is shifted successively along the vertical coordinate.

exponent; that is, the interplay between these correlation parameters contributes to nontrivial scaling properties in the generalized growth system.

To determine the roughness exponent α describing the saturation of the surface fluctuation, usually one needs to calculate the global interfacial width $W(L,t)$ or local interfacial width $w(l,t)$. Unfortunately, due to numerical divergence in the generalized KPZ system, it is not convenient to obtain α using the relation $W(L,t) \sim L^\alpha$ for the system size L in the steady-state regime $t \gg L^z$. However, as we see in the following, an alternative technique to determine the critical exponents of a growing surface is to study the Fourier transform of the interface height in a system of linear size L, $\hat{h}(k,t) = L^{-1/2} \sum_x [h(x,t) - \overline{h}(t)] \exp(ikx)$, where the spatial average of the height has been subtracted. In this representation, the properties of the surface can be investigated by calculating the structure factor or power spectrum $S(k,t) = \langle \hat{h}(k,t)\hat{h}(-k,t) \rangle$, which contains the same information on the system as the local interfacial width or height difference correlation function. For

a self-affine interface, the structure function has a scaling form [24]

$$S(k,t) = k^{-(2\alpha+1)} s(kt^{1/z}), \tag{13}$$

with

$$s(u) = \begin{cases} u^{2(\alpha-\alpha_s)} & \text{if } u \gg 1, \\ u^{2\alpha+1} & \text{if } u \ll 1, \end{cases} \tag{14}$$

where $s(u)$ is a spectral scaling function, and α_s is a spectral roughness exponent. To determine the universal critical exponents, we use the scaling function $S(k,t)k^{(2\alpha+1)}$ against $kt^{1/z}$. All the data collapse nicely onto a universal scaling curve for different growth times when the roughness and dynamic exponents are chosen properly. Thus we can estimate these scaling exponents α and z based on data collapse. Meanwhile, we can also check the scaling exponents obtained independently using the scaling relation $z = \alpha/\beta$.

Figure 4 shows the log-log plot of the structure factor $S(k,t)$ versus wave number k for the generalized KPZ system with
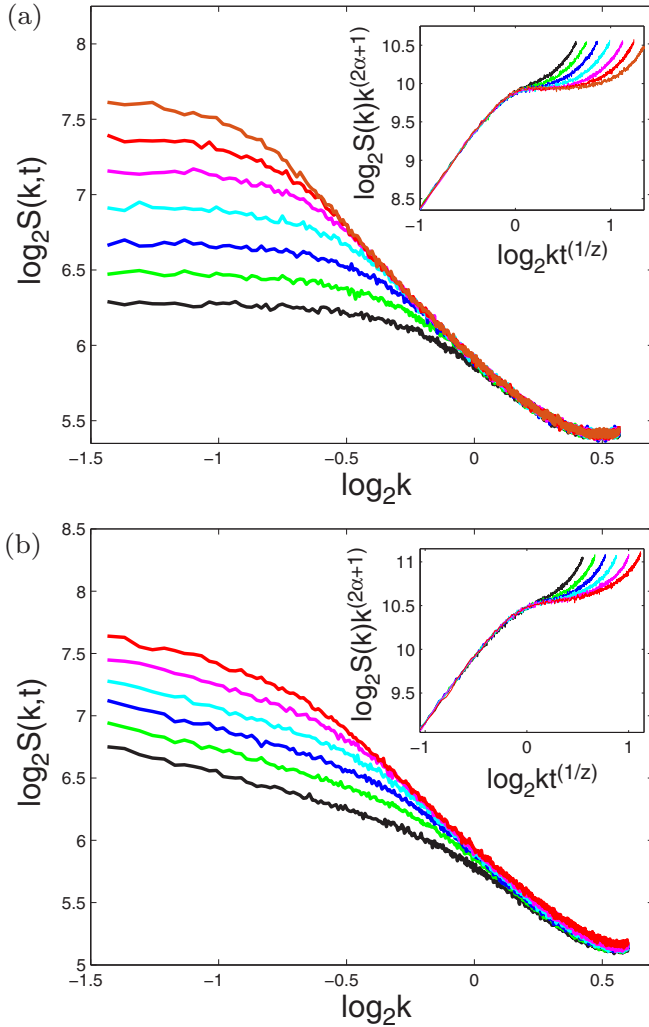
FIG. 5. The structure factor $S(k,t)$ of the growth surface at different growth times from the FKPZ system with $L = 1024$: (a) $\gamma = 1.75$ and $\sigma = 0$ and (b) $\gamma = 1.75$ and $\sigma = 0.25$. All of these results are averaged over 1000 noise realizations. The curves correspond to times from bottom to top: (a) $t = 25, 35, 50, 75,$ 115, 165, and 250; (b) $t = 17, 25, 35, 50, 75,$ and 115. Insets show good data collapses with the critical exponents: (a) $\alpha = 0.440$ and $z = 1.405$ and (b) $\alpha = 0.525$ and $z = 1.375$.

different fractional orders and spatial correlation parameters. Through comparison of systems with different size and growth time, we find that the scaling properties for the structure factor do not change evidently with L and t. Without loss of generality, we choose $L = 1024$ and $t = 100$ in the following simulations. The spectral roughness exponent is calculated for different γ and σ using the scaling relation $S(k,t) \sim k^{-(2\alpha_s+1)}$ in the large wave number regime $kt^{1/z}$. Figure 4(a) shows the double logarithmic plot of $S(k,t)$ versus k for the FKPZ with $\gamma = 1.5$–2.0 and $\sigma = 0$, that is, the fractional KPZ with Gaussian white noise. Figure 4(b) displays the numerical results with $\gamma = 1.5$–2.0 and $\sigma = 0.25$. We find that, when σ is greater than 0.3, the growth instability shows up at a short growth time. Therefore, we choose σ from 0 to 0.3 in the following simulations. Figures 4(c) and 4(d) show numerical

results for the FKPZ ($\sigma = 0$–0.3) with $\gamma = 2.0$ and $\gamma = 1.75$, respectively.

Figures 5(a) and 5(b) exhibit the scaling behavior and data collapse of the structure factor for the FKPZ system ($\gamma = 1.75$) with $\sigma = 0$ and $\sigma = 0.25$, respectively. Measuring the asymptotic decay of the structure factor curves $k^{-(2\alpha_s+1)}$ for long times and small momenta k, we immediately obtain an estimation of the spectral roughness exponent $\alpha_s = 0.438$ ($\sigma = 0$), and $\alpha_s = 0.486$ ($\sigma = 0.25$). Using $S(k,t)k^{(2\alpha+1)}$ versus $kt^{1/z}$, we find that the data collapse is optimal for the critical exponents $\alpha = 0.440$ and $z = 1.405$ ($\gamma = 1.75$ and $\sigma = 0$), and the results are shown in the inset of Fig. 5(a). Similar to the case of $\gamma = 1.75$, we also find that the global roughness exponent obtained by a good data collapse with different γ and $\sigma = 0$ is in excellent agreement with the corresponding spectral roughness exponent. These results provide numerical evidence that the normal Family-Vicsek scaling relation still applies, and anomalous behavior cannot occur in this special case of the FKPZ system ($\gamma = 1.5$–2.0 and $\sigma = 0$). In Fig. 5(b), we choose parameters with $\gamma = 1.75$ and $\sigma = 0.25$ as a general example of the generalized KPZ system. Here, the critical exponents used for the best data collapse are $\alpha = 0.525$ and $z = 1.375$. Interestingly, our results show that, when $\sigma \neq 0$, the global roughness exponent with different γ is larger than the corresponding spectral roughness exponent, i.e., $\alpha > \alpha_s$. Therefore, these results imply that the FKPZ system with $\sigma > 0$ does not display normal scaling behavior and agree with the case of intrinsic anomalous roughening [24].

Following the above steps of data collapse, we then proceed to estimate the global roughness and dynamical exponents in the FKPZ system with different γ and σ. The values of critical exponents, and the comparisons with some relevant theoretical predictions, are shown in Fig. 6. In the nonlinear FKPZ system, the results show that the comparison between the numerical results and theoretical predictions is rather nontrivial. First, the global roughness exponent increases gradually with the increasing fractional order when $\sigma = 0.25$. More specifically, $\alpha = 0.465 \sim 0.558$ ($\gamma = 1.5$–2.0). And the critical exponent depends weakly on γ when $\sigma = 0$, that is, $\alpha = 0.430 \sim 0.475$ ($\gamma = 1.5$–2.0). This difference implies that, by introducing the spatially correlated noise into the FKPZ equation, the interplay of these correlation parameters also plays a role in the scaling behavior of the FKPZ system in the saturated growth regimes [see Fig. 6(a)]. Meanwhile, the roughness exponent has weak dependence on σ when γ is constant, and the values of α ($\gamma = 1.75$, $\sigma = 0$–0.3) are smaller than the corresponding values when $\gamma = 2.0$ [see Fig. 6(b)]. For the two extreme cases of the FKPZ system ($\gamma = 2.0$, $\sigma = 0$–0.3 and $\gamma = 1.5$–2.0, $\sigma = 0$), the computed global roughness exponent agrees well with the theoretical predictions of Refs. [9,16]. Slightly different from α versus γ or σ, the dynamic exponent is independent of the correlation parameters [see Figs. 6(c) and 6(d)]. When $\gamma = 1.5$–2.0 and $\sigma = 0$, the values of z agree with the theoretical results [16]. And for the other special case ($\gamma = 2.0$), our results differ slightly from the theoretical prediction [9]. However, for the linear FEW system, the roughness exponent relies dramatically on the long-range correlation parameters, i.e., γ and σ [see Figs. 6(a) and 6(b)]. And the global roughness exponent equals approximately the corresponding spectral exponent.
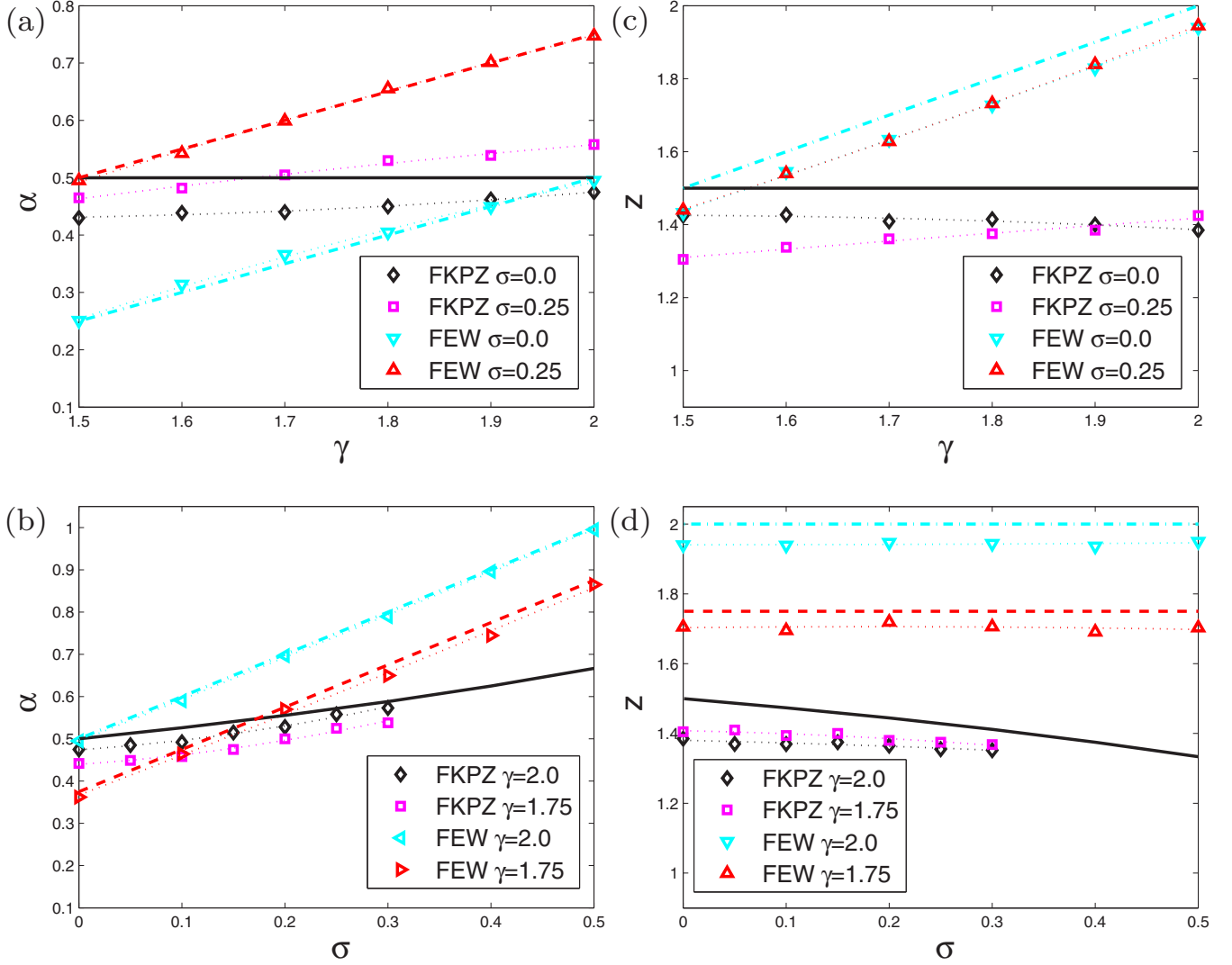
FIG. 6. The roughness and dynamic exponents for the FKPZ and FEW equations in various parameter regimes: (a) α versus γ, (b) α versus σ, (c) z versus γ, and (d) z versus σ. In (a) and (c), the theoretical predictions for the FKPZ ($\gamma = 1.5$–2.0, $\sigma = 0$) [16], FEW ($\gamma = 1.5$–2.0, $\sigma = 0$), and FEW ($\gamma = 1.5$–2.0, $\sigma = 0.25$) equations are solid, dot-dashed, and dashed lines, respectively. And the solid, dot-dashed, and dashed lines in (b) and (d) indicate the predictions for the FKPZ ($\gamma = 2.0$, $\sigma = 0$–0.5) [9], FEW ($\gamma = 2.0$, $\sigma = 0$–0.5), and FEW ($\gamma = 1.75$, $\sigma = 0$–0.5) equations, respectively.

Thus, anomalous scaling could not occur in the linear growth system. Interestingly, the dynamic exponent depends strongly on the fractional order [see Fig. 6(c)] but does not change with the spatial correlation parameter [see Fig. 6(d)]. All of these values for the FEW system are in good agreement with the theoretical results based on power counting. Furthermore, we also find that the scaling exponents obtained independently could basically satisfy the relation $z = \alpha/\beta$ for both the linear FEW and the nonlinear FKPZ systems.

IV. DISCUSSIONS AND CONCLUSIONS

In our simulation, we find that numerical divergence always exists in the discretized version of the nonlinear fractional growth system. On the contrary, no divergence appears in the linear fractional case. The apparent singularity in Eq. (4), indicated by a rapid growth of the height variable, is found to occur randomly in finite growth time [see Figs. 7(a)–7(c)].

It is impossible to follow numerically the evolution of the nonlinear system beyond the time at which singularity occurs. Interestingly, a similar behavior is also found in the case of the discrete stochastic models describing growing surfaces. It was said that there is a genuine instability intrinsic to the discretized continuum growth system with nonlinearities [25,26].

To suppress the instability induced by the nonlinear term of the growth equations, Dasgupta *et al.* [25] suggested that the squared gradient in the equation should be replaced by an exponentially decreasing function; e.g., $(\nabla h)^2$ in the KPZ equation is replaced by $f((\nabla h)^2)$, where $f(x) = (1 - e^{-cx})$ with c being an adjustable parameter. This scheme avoids rapid growth caused by the large local height difference, which is the origin of the instability. In the modified discretized growth equation, the nonlinear term is still estimated from the nearest neighbors in all spatial directions. It was said that this method of suppressing instability does not change scaling exponents and other universal quantities [25]. In this work, we adopt the
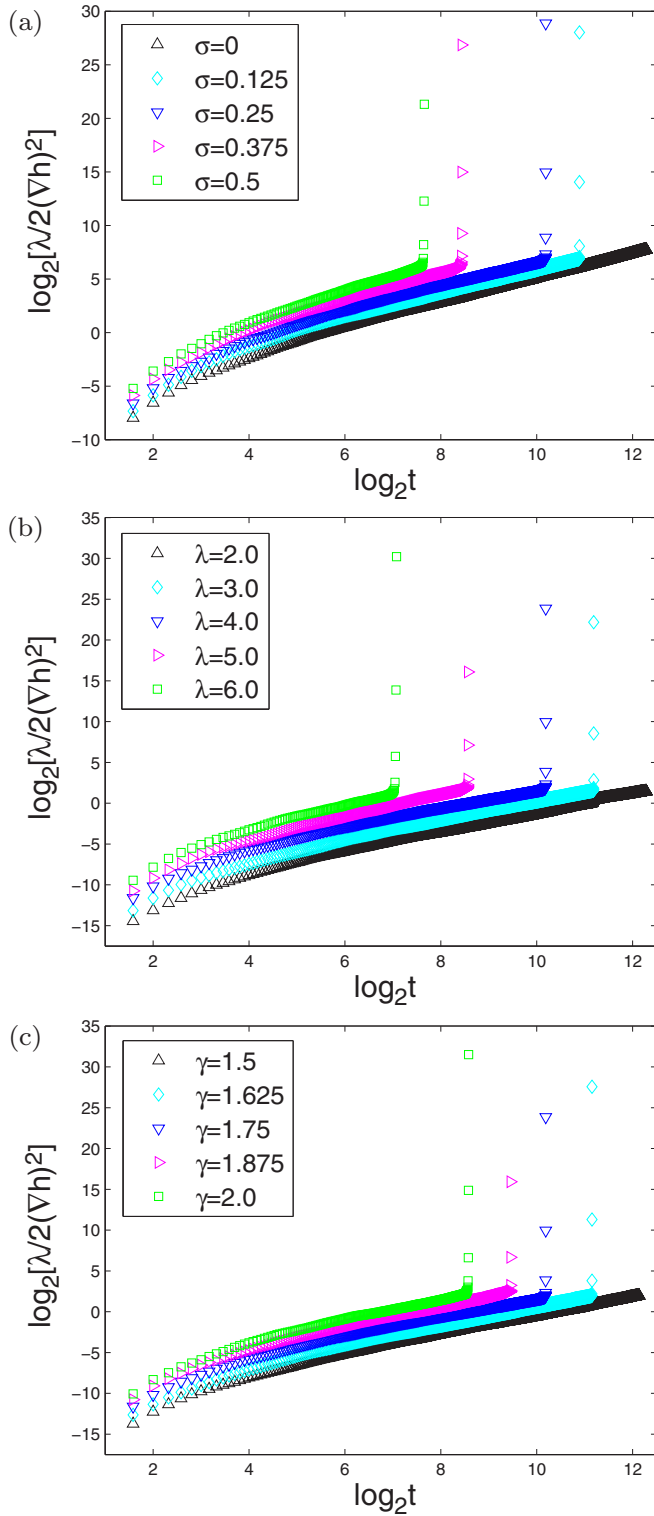
FIG. 7. The nonlinear term versus growth time for the FKPZ equation (a) with different σ ($\lambda = 4$, $\gamma = 1.75$), (b) with different λ ($\gamma = 1.75$, $\sigma = 0.25$), and (c) with different γ ($\sigma = 0.25$, $\lambda = 4$).

scheme mentioned above in order to suppress the annoying numerical divergence in the FKPZ system. Unfortunately, except for several special cases, this control strategy could not effectively suppress the instability in the nonlinear generalized growth equation (4).

In the following, we discuss the main factors leading to the growth instability. The dynamical growth processes are simulated with the original generalized KPZ equation. It can be seen that, in the early time, the fractional growth displays normal surface morphology, and there are no obvious mounds formed on the surfaces. With the increase of the growth time, the lateral length of the surface features becomes larger, and some grooves appear and become coarse, followed by a large isolated groove, which leads to instability eventually. It should be pointed out that this instability is not a consequence of unsuitably large time steps, but an intrinsic feature of the discretization of the normal KPZ and other nonlinear equations [25–27].

To display the unstable dynamical processes, the time evolution of the nonlinear term is calculated through altering the values of three potential parameters σ, λ, and γ (see Fig. 7). Interestingly, altering any of these parameters leads to similar growth instability, and the instability onset arrives early with increasing parameter values.

Through comparing directly these numerical results, we notice that, for a given parameter, the instability of the nonlinear term has different dependence on the order parameter. In Figs. 7(a)–7(c), the average value of the nonlinear term for Eq. (4) is shown as a function of the growth time:

(i) When λ and γ are fixed ($\lambda = 4.0$ and $\gamma = 1.75$), with increasing σ, the apparent singularity indicated by a rapid growth of the nonlinear term occurs at an earlier time [see Fig. 7(a)].

(ii) Figure 7(b) shows that, when σ and γ are fixed ($\sigma = 0.25$ and $\gamma = 1.75$), the singularity of the growth shows up at different time with different λ. More specifically, the onset of the instability always becomes earlier with increasing λ.

(iii) When σ and λ are chosen as constants ($\sigma = 0.25$ and $\lambda = 4.0$), by varying γ, we also find a similar unstable growth [see Fig. 7(c)].

Therefore, we conclude that the chosen parameters σ, λ, and γ could independently affect the growth instability in the FKPZ system. We also find that, under certain circumstances (e.g., $\sigma = 0$, or $\lambda \leqslant 2$, or $\gamma = 1.5$), the numerical instability does not come up in the long-time simulation of Eq. (4).

We noticed that the random-matrix theory is closely linked to growth phenomena over the recent years [28–30]. Both theoretical and numerical evidences have been gathered, showing that the growth systems in the KPZ universality class share not only the values of the scaling exponents, but also the full probability distribution of the interface fluctuations. For the (1+1)-dimensional KPZ class, including the discrete models [28], the related experiments [31], and the KPZ equation itself [32], it is believed that the interface fluctuations follow the Tracy-Widom (TW) probability distribution function associated with large random matrices. Therefore, it would be of interest to study probability distributions of the height in the FKPZ equation discussed here. Perhaps such a program could further identify the universal properties hiding behind the generalized growth system beyond the standard KPZ case.

In summary, we have investigated the time evolution of the roughness in the solution of the (1+1)-dimensional FKPZ equation driven by spatially correlated noise based on an explicit finite-difference approximation of the Riesz-type

fractional derivative. We computed the critical exponents of the interfacial width and structure factor with various long-range correlation parameters. Roughly speaking, for the nonlinear FKPZ system, the scaling exponents have strong dependence on noise correlation parameter and weak dependence on the fractional order. Moreover, we also noticed that when introducing the correlated noise and fractional order together, the interplay between these correlation parameters affects evidently the scaling behavior of the generalized growth system. In the two extreme cases of the FKPZ system, the critical values are consistent with those obtained through scaling analysis [9] and the SCE approach [16]. Compared with the original KPZ with correlated noise and FKPZ with Gaussian white noise, the FKPZ system in the presence of spatially correlated noise has stronger numerical instability. As a linear case of the FKPZ system, the numerical results based on the FEW equation are in excellent agreement with previous theoretical analysis [4,15]. Unlike in the FKPZ equation, the scaling exponents in the linear fractional growth system depend strongly on the correlation parameters. This class of linear fractional growth processes demonstrates an interesting type of continuous universality. Furthermore, due to the trivial scaling properties of the FKPZ system when $\sigma = 0$, the estimated values of the global roughness exponents are approximately equal to the spectral roughness ones, i.e., $\alpha \sim \alpha_s$. The results provide the numerical evidence that

anomalous behavior does not occur in the FKPZ system driven by Gaussian white noise. However, when $\sigma \neq 0$, the results show that the estimated global roughness exponent is larger than the corresponding spectral roughness exponent, which satisfies the case of intrinsic anomalous roughening [24]. Therefore, we assume that the FKPZ driven by spatially correlated noise exhibits nontrivial scaling properties, and anomalous scaling behavior can occur in this kind of growth system with long-range correlations. This conclusion is also consistent with the theoretical arguments by López *et al.* that disorder or nonlocal effects must be responsible for the occurrence of intrinsic anomalous roughening [33]. Through extensive numerical simulations, our results show that the noise correlation parameter, the nonlinear coefficient, and the fractional order all play important roles in the rapid growth of instability. How to suppress effectively this instability needs further research.

ACKNOWLEDGMENTS

[1] A.-L. Barabási and H. E. Stanley, *Fractal Concepts in Surface Growth* (Cambridge University Press, Cambridge, UK, 1995).

[2] P. Meakin, Phys. Rep. **235**, 189 (1993).

[3] T. Halpin-Healy and Y. C. Zhang, Phys. Rep. **254**, 215 (1995).

[4] J. Krug, Adv. Phys. **46**, 139 (1997).

[5] M. Kardar, G. Parisi, and Y. C. Zhang, Phys. Rev. Lett. **56**, 889 (1986).

[6] F. Family and T. Vicsek, J. Phys. A: Math. Gen. **18**, L75 (1985).

[7] R. Metzler and J. Klafter, J. Phys. A: Math. Gen. **37**, R161 (2004).

[8] E. Medina, T. Hwa, M. Kardar, and Y.-C. Zhang, Phys. Rev. A **39**, 3053 (1989).

[9] H. G. E. Hentschel and F. Family, Phys. Rev. Lett. **66**, 1982 (1991).

[10] C.-K. Peng, S. Havlin, M. Schwartz, and H. E. Stanley, Phys. Rev. A **44**, R2239 (1991).

[11] E. Katzav and M. Schwartz, Phys. Rev. E **60**, 5677 (1999).

[12] S. Mukherji and S. M. Bhattacharjee, Phys. Rev. Lett. **79**, 2502 (1997).

[13] A. Kr. Chattopadhyay, Phys. Rev. E **60**, 293 (1999).

[14] E. Katzav, Phys. Rev. E **68**, 046113 (2003).

[15] J. A. Mann and W. A. Woyczynski, Physica A **291**, 159 (2001).

[16] E. Katzav, Phys. Rev. E **68**, 031607 (2003).

[17] I. Podlubny, *Fractional Differential Equations* (Academic Press, New York, 1999).

[18] G. L. Kellogg, Phys. Rev. Lett. **72**, 1662 (1994).

[19] M. Schwartz and S. F. Edwards, Europhys. Lett. **20**, 301 (1992).

[20] S. F. Edwards and D. R. Wilkinson, Proc. R. Soc. London Ser. A **381**, 17 (1982).

[21] Q. Yang, F. Liu, and T. Turner, Appl. Math. Model **34**, 200 (2010).

[22] H. Xia, G. Tang, D. P. Hao, and Z. P. Xun, J. Phys. A: Math. Theor. **45**, 295001 (2012).

[23] E. Katzav and M. Schwartz, Europhys. Lett. **95**, 66003 (2011); Phys. Rev. Lett. **107**, 125701 (2011).

[24] J. J. Ramasco, J. M. López, and M. A. Rodríguez, Phys. Rev. Lett. **84**, 2199 (2000).

[25] C. Dasgupta, J. M. Kim, M. Dutta, and S. Das Sarma, Phys. Rev. E **55**, 2235 (1997).

[26] B. Chakrabarti and C. Dasgupta, Phys. Rev. E **69**, 011601 (2004).

[27] V. G. Miranda and F. D. A. Aarao Reis, Phys. Rev. E **77**, 031134 (2008).

[28] M. Prähofer and H. Spohn, Phys. Rev. Lett. **84**, 4882 (2000).

[29] T. Kriecherbauer and J. Krug, J. Phys. A: Math. Theor. **43**, 403001 (2010).

[30] S. N. Santalla, J. Rodríguez-Laguna, T. LaGatta, and R. Cuerno, New J. Phys. **17**, 033018 (2015).

[31] K. A. Takeuchi, M. Sano, T. Sasamoto, and H. Spohn, Sci. Rep. **1**, 34 (2011).

[32] T. Sasamoto and H. Spohn, Phys. Rev. Lett. **104**, 230602 (2010).

[33] J. M. López, M. Castro, and R. Gallego, Phys. Rev. Lett. **94**, 166103 (2005).